Combining tilt derivative filters: new approaches to enhance magnetic anomalies

Castro, F.R., UFPR; Oliveira, S.P.*, UFPR; de Souza, J., Secretary of Education/PR; Ferreira, F.J.F., UFPR

Abstract

We expand the concept of two earlier enhancement techniques based on the tilt angle. The proposed method is based on the addition and subtraction of vertical and horizontal tilt derivatives, TDR+TDX and TDR–TDX, respectively. TDR+TDX has the property of not varying over the causative bodies, like plateaus, while TDR–TDX produces peaks over the bodies and does not vary where there are no sources. The proposed methods are applied to synthetic and real data, and provide more clearly the locations of edges and centers of the sources with respect to TDR and TDX.

Introduction

Enhancement methods based on first-order derivatives of gravity and magnetic fields are commonly employed to locate edges and centers of causative sources. These techniques are robust in the sense that they can cope with low-quality data (Pilkington & Tschirhart, 2017).

Some of the classical methods of this class are the amplitude of the analytical signal (ASA - Nabighian, 1972,1974; Roest et al., 1992) and the total horizontal gradient (THDR - Cordell & Grauch, 1985).

Later on, several methods have resorted to normalization in order to balance low and high amplitudes due to shallow and deep sources, respectively. Among these, we emphasize the Tilt Angle (TDR - Miller & Singh, 1994), the Horizontal Tilt Angle (TDX - Cooper & Cowan, 2006), and the Theta Map (θ - Wijns et al., 2005). These approaches have been extended to employ higher-order derivatives as well (Verduczo et al., 2005; Ferreira et al., 2013).

It is well known that some of these methods are equivalent to each other (e.g., Pilkington & Tschirhart, 2017). In particular, Ferreira et al (2013) observed that |TDR| = θ, as well as |TDR| = π/2-TDX.

In this work we explore the latter relation, which grants special properties to two particular combinations of these filters: TDR+TDX and TDR-TDX.

As we shall see next, TDR+TDX represents an improvement over TDX in the sense that its peak values are located not only near the edges of the sources, but over the whole sources, resulting in a plateau over them. Likewise, TDR-TDX not only produces a peak over the center of the bodies as TDR, but also generates a plateau over the regions in absence of sources. The plateaus provided by these combined techniques render the potential field easier to interpret.

Theory

Let us recall that the TDR and TDX filters are respectively defined as follows:

$$\mathrm{TDR} = \tan^{-1}\left(\frac{\mathrm{M_z}}{\mathrm{M_h}}\right), \qquad \mathrm{TDX} = \tan^{-1}\left(\frac{\mathrm{M_h}}{|\mathrm{M_z}|}\right),$$

where M_z and M_h are vertical and horizontal derivatives of the anomaly M. Both relations equalize the field responses due to the characteristics of the arctangent, which limits the range to -π/2 to π/2. Moreover, since $\tan^{-1}(-x) = -\tan^{-1}(x)$, it follows that

$$|\mathrm{TDR}| = \tan^{-1}\left(\frac{|\mathrm{M_z}|}{\mathrm{M_h}}\right) = \cot^{-1}\left(\frac{\mathrm{M_h}}{|\mathrm{M_z}|}\right),$$

thus, tan(TDX)=cot(|TDR|). If M_z = 0, then TDX= π/2 and |TDR|=0, i.e., |TDR| = π/2-TDX. Otherwise,

$$0 = \tan(\mathrm{TDX}) - \cot(|\mathrm{TDR}|) = \frac{\cos(\mathrm{TDX} + |\mathrm{TDR}|)}{\cos(\mathrm{TDX})\sin(|\mathrm{TDR}|)},$$

which implies cos(TDX+|TDR|) = 0, and again |TDR| = π/2-TDX. This relation can be written as follows:

TDR+TDX = π/2, if TDR>0

TDR-TDX= -π/2, if TDR<0,

Since TDR is positive over a source and negative elsewhere (Miller & Singh, 1994), it turns out that the combined filter TDR+TDX provides a plateau with value +π/2 over the sources, whereas TDR-TDX produces plateaus with value -π/2 in regions where sources are not expected.

Synthetic example

To illustrate the properties of the proposed methods, a synthetic model with three equally spaced prisms was generated to simulate parallel dyke-like bodies with different depths to top (Fig. 1). The model parameters are shown in Table 1. The strength, declination and inclination of the induced field vector are 57000 nT, 0, and 90 degrees, respectively, and no remanent magnetization was considered.

Table 1 - Spatial and physical parameters of the synthetic model. X, Y, Z are the coordinates of the prisms.

Prism	**X (km)**	**Y (km)**	**Z (km)**	**Length (km)**	**Width (km)**	**Thickness (km)**
A	5	10	0.2	18	1	18
B	10	10	0.4	18	1	18
C	15	10	0.6	18	1	18

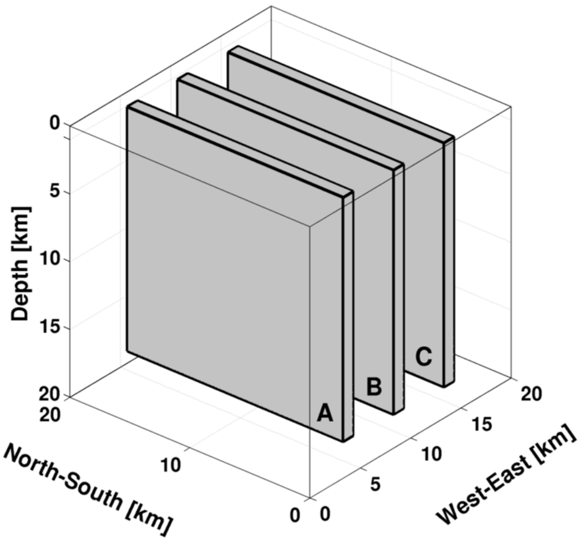

Figure 1 – 3D view of parallel dyke-like body model.

Figure 2 shows the magnetic anomaly, whereas Figures 3 and 4 show TDR±TDX. The plateaus over the sources (TDR+TDX) and out of sources (TDR-TDX) and the peaks of TDR-TDX are located at the bodies' centers, as in TDR.

The profiles at y=10km are gathered in Fig. 10. Note that TDR+TDX fills in a plateau between the peaks of TDX (Fig. 10c), which makes the source locations more visible.

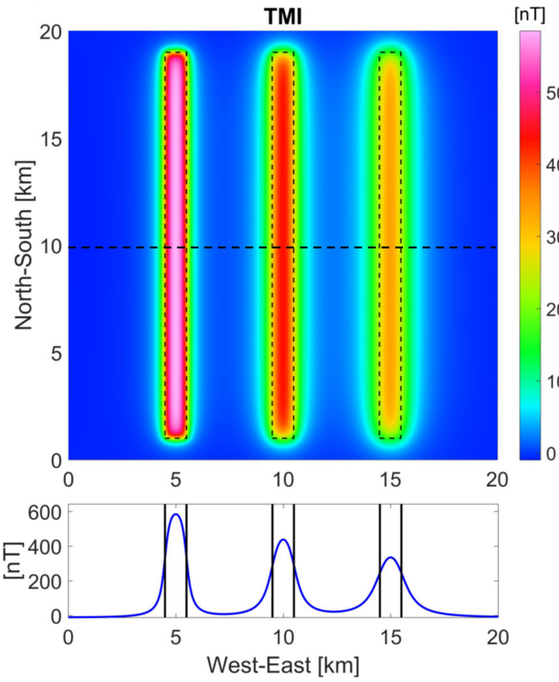

Figure 2 – Total magnetic intensity of the synthetic example and profile at y=10km (dashed line).

Moreover, TDR-TDX improves TDR by flattening its response away from the sources (Fig. 10d). The resulting profile represents the sources better also than the first-order derivatives M_h (i.e., THDR) and M_z, shown in Fig. 10b.

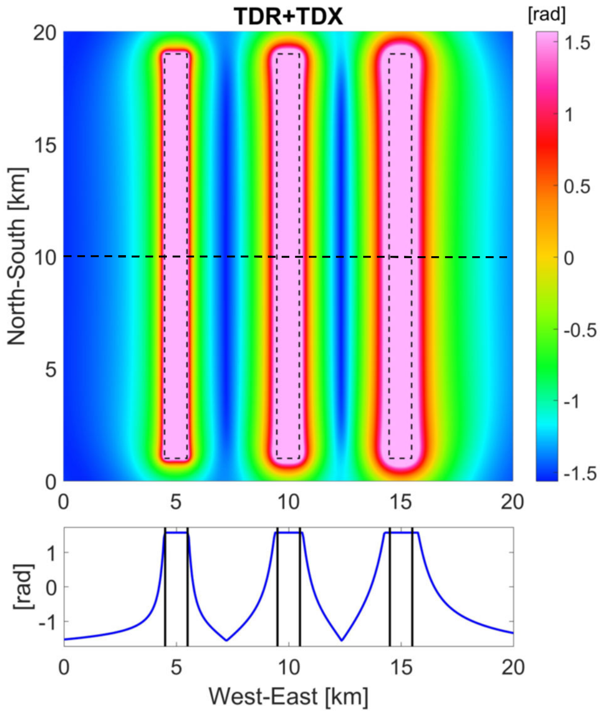

Figure 3 – TDR+TDX of the data in Fig. 3 and profile at y=10km.

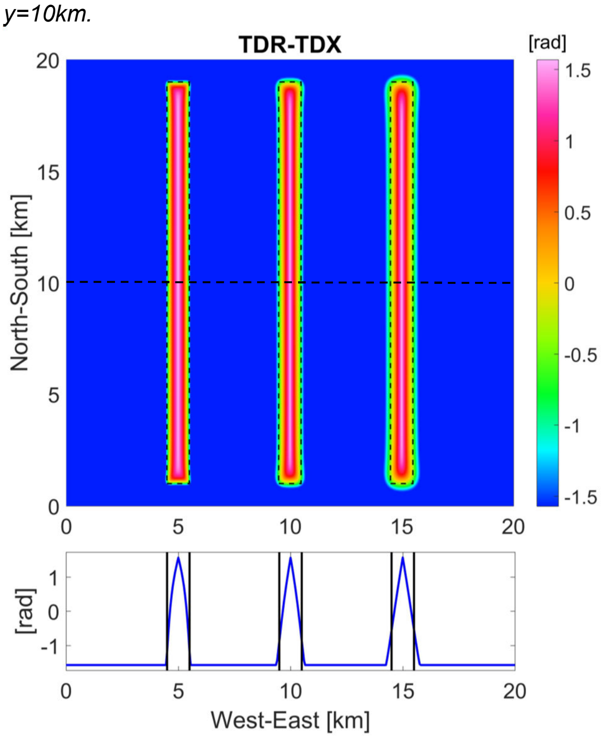

Figure 4 – TDR-TDX of the data in Fig. 3 and profile at y=10km.

Field example

Both combined filters are tested in field data from the Paraná - Santa Catarina Aerogeophysical Project (CPRM, 2011) in the portion of the Ponta Grossa Arch, an expressive dyke swarm in southern Brazil. The aeromagnetic data were acquired along north-south flight lines spaced at 500 m, with a mean terrain clearance of 150 m. The tie lines had 10 km spacing.

Figure 5 shows the total magnetic intensity of the field data reduced to the pole, whereas Figs. 6-9 show the corresponding maps of TDR, TDX, TDR+TDX and TDR-TDX, respectively.

TDR+TDX predicts a high density of sources, with few regions free from interference (-π/2). On the other hand, TDR-TDX focuses on the centers of the sources and seems to remain insensitive to interference zones.

Note that the dykes in the SW portion of the TMI map (Fig.5) are blurred by a single anomaly pattern. On the other hand, the dykes are clearly delineated in the TDR+TDX and TDR-TDX maps (Figs. 8 and 9).

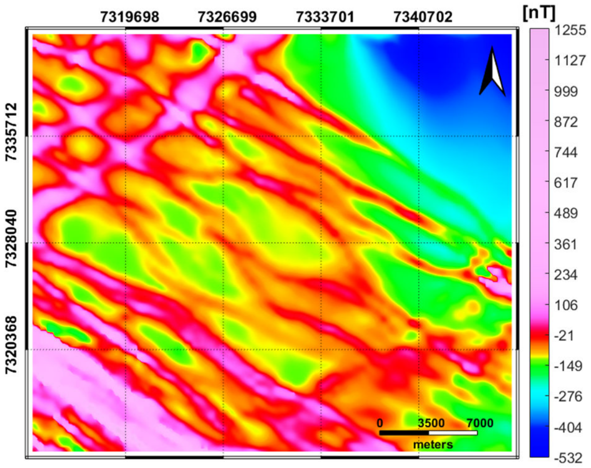

Figure 5 – TMI of the field data reduced to the pole.

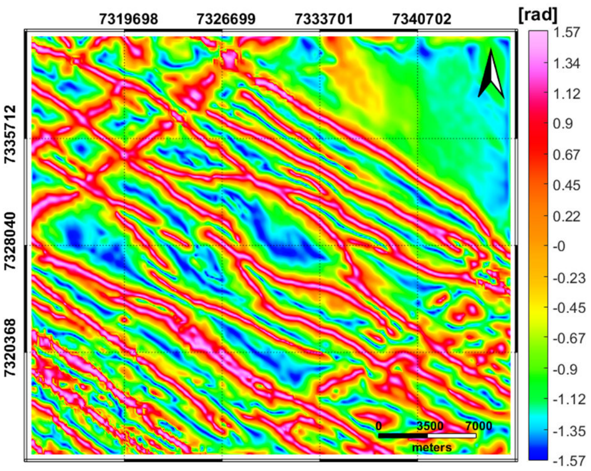

Figure 6 – TDR of the data in Fig. 5.

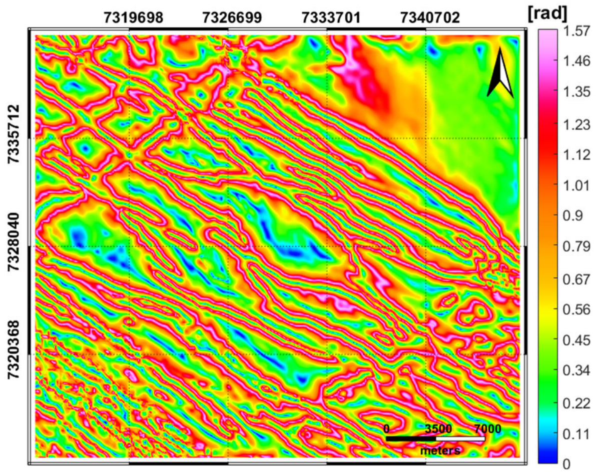

Figure 7 – TDX of the data in Fig. 5.

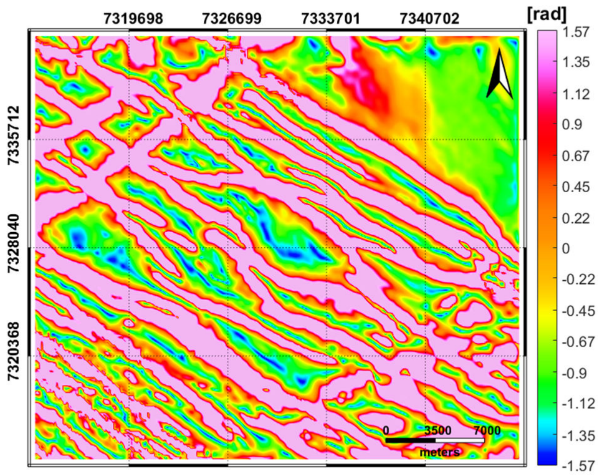

Figure 8 – TDR+TDX of the data in Fig. 5.

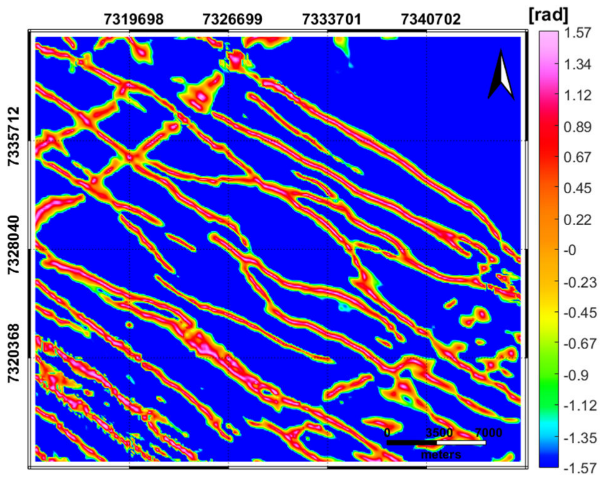

Figure 9 – TDR-TDX of the data in Fig. 6.

Conclusions

In this preliminary study, we have verified that simple combinations of well-known tilt derivative filters have shown to improve the focus on the edges and centers of the sources, in both synthetic and field data. Additional testing is needed to assess the robustness with noisy data and non-vertical magnetization.

The proposed filters naturally inherit some limitations from the primary ones. Both TDR+TRX and TDR-TRX products spread those lateral limits according to depth increasing, for example, for deep sources the limits of body edges will appear greater than actual edges.

Acknowledgments

The authors thank Companhia de Pesquisa de Recursos Minerais for permission to use the aeromagnetic data. F. J. F. Ferreira and S. P. Oliveira are supported by CNPq (grants 306978/2015-6 and 313100/2017-9, respectively).

References

Cooper, G. R. J. & Cowan, D. R., 2006, Enhancing potential field data using filters based on the local phase: Computers & Geosciences, 32: 1585-1591.

Cordell, L. & Graunch, V. J. S., 1985. Mapping basement magnetization zones from aeromagnetic data in the San Juan Basin, New Mexico. In: Hinze WJ (Ed). The Utility of Regional Gravity and Magnetic Anomalies Maps. Society of Exploration Geophysicists: 181-197.

CPRM. 2011. Paraná – Santa Catarina Aerogeophysical Project. (CPRM, Geological Survey of Brazil).

Ferreira, F. J. F., de Souza, J., Bongiolo, A. B. S. & de Castro, L.G., 2013. Enhancement of the total horizontal gradient of magnetic anomalies using the tilt angle. Geophysics, 78: J33-J41.

Miller, H. G. & Singh, V., 1994, Potential field tilt - A new concept for location of potential field sources: Journal of Applied Geophysics, 32: 213–217.

Nabighian, M. N., 1972. The analytic signal of two-dimensional magnetic bodies with polygonal cross section: Its properties and use for automated anomaly interpretation. Geophysics, 37: 507-517.

Nabighian, M. N., 1974. Additional comments on the analytic signal of two-dimensional magnetic bodies with polygonal cross-section. Geophysics, 39: 85-92.

Pilkington, M. & Tschirhart, V., 2017, Practical considerations in the use of edge detectors for geologic mapping using magnetic data: Geophysics, 82: J1-J8.

Roest, W. R, Verhoef, J. & Pilkington, M., 1992. Magnetic interpretation using the 3-D analytic signal, Geophysics, 57:116-125.

Verduzco, B, Fairhead, J. D., Green, C.M. & Mackenzie, C., 2004. New insights into magnetic derivatives for structural mapping. The Leading Edge, 23: 116-119.

Wijns, C., Perez, C. & Kowalczyk, P., 2005. Theta map: Edge detection in magnetic data. Geophysics, 70: L39-L43.

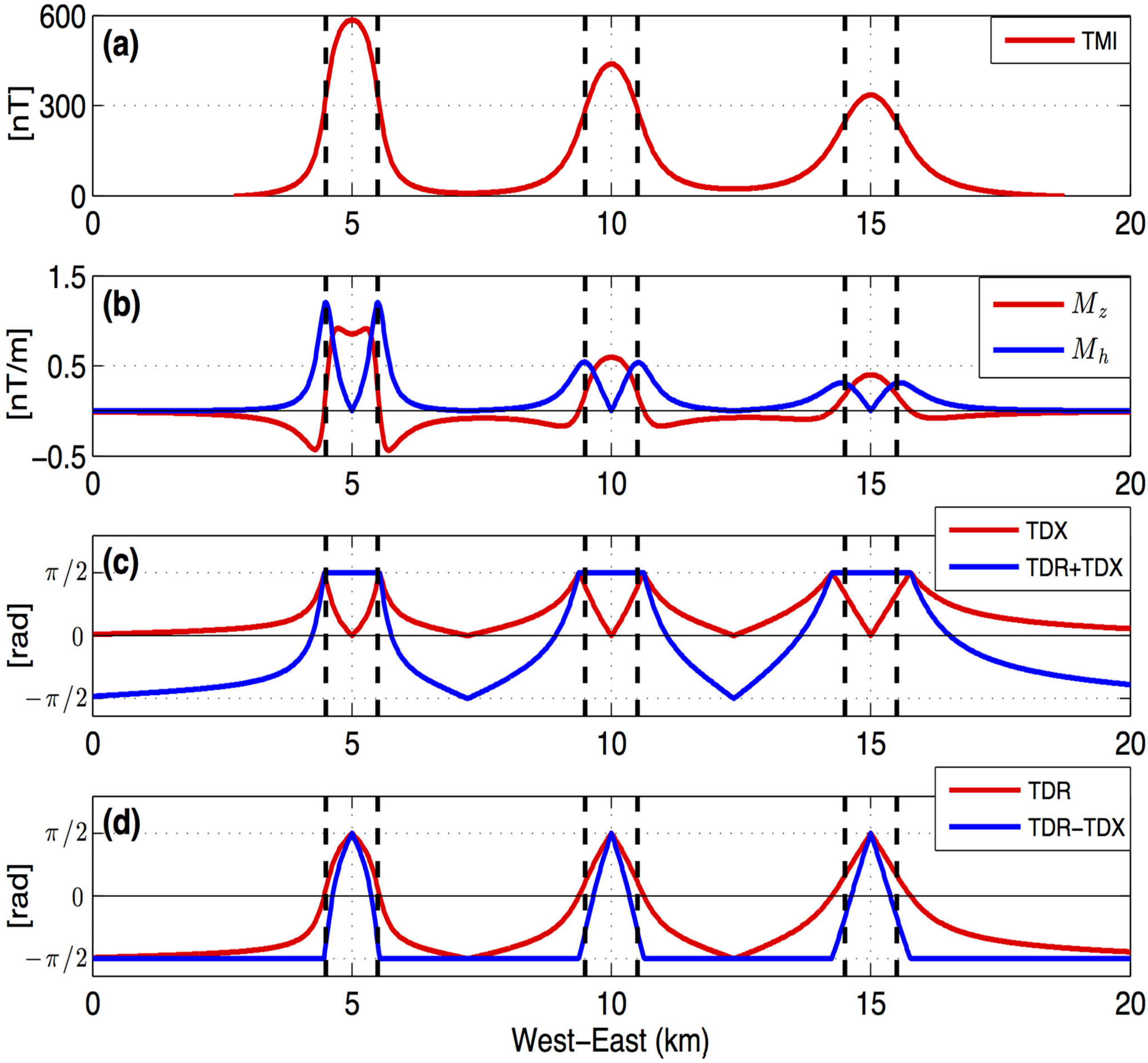

Figure 10 – Profiles at y=10km: (a) TMI profile (extracted from Fig. 2); (b) first-order derivatives (Mz and Mx); (c) TDX and TDR+TDX; (d) TDR and TDR-TDX.